Available online at www.sciencedirect.com
ScienceDirect
Control Engineering Practice 16 (2008) 1109–1119
CONTROL ENGINEERING PRACTICE
www.elsevier.com/locate/conengprac

Power system dynamic stability and voltage regulation enhancement using an optimal gain vector

Hassan Bevrani[a,*], Takashi Hiyama[b], Yasunori Mitani[c]

[a]Department of Electrical and Computer Engineering, University of Kurdistan, Sanandaj, Kurdistan, Iran
[b]Department of Electrical and Computer Engineering, Kumamoto University, Kumamoto, Japan
[c]Department of Electrical Engineering, Kyushu Institute of Technology, Kita-Kyushu, Japan

Received 12 June 2007; accepted 14 January 2008
Available online 4 March 2008

Abstract

This paper addresses a control methodology to enhance power system dynamic stability and voltage regulation by augmenting existing generator controls (conventional PSS and AVR) using an optimal static gain vector. The control design problem is reduced to finding a new control loop including a simple fixed gain vector. In order to optimal tune gain elements, the problem is formulated via an H_∞ static output feedback (H_∞-SOF) control technique, and the solution is easily found using an iterative linear matrix inequalities (ILMI) algorithm. Real-time experiments have been performed for a longitudinal four-machine infinite-bus system on the Analog Power System Simulator at the Research Laboratory of the Kyushu Electric Power Co. The proposed robust technique is shown to maintain the robust performance and minimize the effects of disturbances.

Keywords: Power system stabilizer; Voltage regulation; H_∞ control; Static output feedback; LMI

1. Introduction

Power systems continuously experience changes in operating conditions due to variations in generation/load and a wide range of disturbances. Power system stability and voltage regulation have been considered an important problem for secure system operation over many years (Kundur et al., 2004). Currently, because of expanding physical setups, functionality and complexity of power systems, the mentioned problems become more significant than in the past. That is why in recent years a great deal of attention has been paid to application of advanced control techniques to power systems.

Conventionally, the automatic voltage regulation and power system stabilizer (AVR–PSS) design is considered as a sequential design including two separate stages. Firstly, the AVR is designed to meet the specified voltage regulation performance and then the PSS is designed to satisfy the stability and required damping performance. It is known that stability and voltage regulation are ascribed to different model descriptions, and it has been long recognized that AVR and PSS have inherent conflicting objectives (Law, Hill, & Godfrey, 1994a, 1994b; Venikov & Stroev, 1971).

In the last two decades, some studies have considered an integrated design approach to AVR and PSS design using domain partitioning (Venikov & Stroev, 1971), robust pole-replacement (Soliman & Sakar, 1988) and adaptive control (Malik, Hope, Gorski, Uskakov, & Rackevich, 1986). Moreover, several control methods have recently been made to coordinate the various requirements for stabilization and voltage regulation within the one new control structure (Bevrani & Hiyama, 2006; Guo, Hill, & Wang, 2001; Heniche, Bourles, & Houry, 1995; Wang & Hill, 1996; Yadaiah, Kumar, & Bhattacharya, 2004).

Although most of these approaches have been proposed based on new contributions in modern control systems, they are not well suited to meet the design objectives in a real multi-machine power system because of following two main reasons: (i) The complexity of control structure, numerous unknown design parameters and neglecting real

*Corresponding author. Tel.: +98 871 6624774; fax: +98 871 6660073.
E-mail address: bevrani@uok.ac.ir (H. Bevrani).

0967-0661/$ - see front matter © 2008 Elsevier Ltd. All rights reserved.
doi:10.1016/j.conengprac.2008.01.001

constraints can be frequently seen in the most of new suggested techniques. While in real world power systems, usually controllers with simple structure are desirable. That is why electric industry still uses the simple PI, PID and Lead-lag controllers that their parameters are commonly tuned based on classical, experiences and trial-and-error approaches. (ii) Experience shows that although the conventional PSS and AVR systems are incapable of obtaining good dynamical performance for a wide range of operating conditions and disturbances, the electric industry is too conservative to open the conventional control loops and test the novel/advanced controllers because of some probable risks, bugs and/or having a complex structure.

In response to above problems, this paper presents a methodology to enhance the stability and voltage regulation of existing real power system without opening their conventional PSS and AVR devices. The methodology provides a simple gain vector in parallel with the conventional control devices. The design objectives are formulated via an H_∞-SOF (H_∞ static output feedback) control problem and the optimal static gains are obtained using an ILMI (iterative linear matrix inequalities) algorithm. The preliminary step of this work has been presented in Bevrani and Hiyama (2006).

The controller proposed in this paper uses the measurable signals and has merely proportional gains; so gives considerable promise for implementation, especially in a multi-machine system. In fact the proposed control strategy attempts to make a bridge between the simplicity of control structure and robustness of stability and performance to satisfy the simultaneous AVR and PSS tasks.

To demonstrate the efficiency of the proposed control method, some real time nonlinear laboratory tests have been performed on a four-machine infinite-bus system using the large scale Analog Power System Simulator at the Research Laboratory of the Kyushu Electric Power Company (Japan). The obtained results are compared with a conventional AVR–PSS system.

2. Proposed control strategy

2.1. A background on H_∞-SOF control design

This section gives a brief overview for the H_∞-SOF control design. Consider a linear time invariant system $G(s)$ with the following state-space realization.

$$G_i(s):\ \begin{aligned}\dot{x}_i &= A_i x_i + B_{1i} w_i + B_{2i} u_i,\\ z_i &= C_{1i} x_i + D_{12i} u_i,\\ y_i &= C_{2i} x_i,\end{aligned} \tag{1}$$

where x_i is the state variable vector, w_i is the disturbance and area interface vector, u_i is the control input vector, z_i is the controlled output vector and y_i is the measured output vector. The A_i, B_{1i}, B_{2i}, C_{1i}, C_{2i} and D_{12i} are known real matrices of appropriate dimensions.

The H_∞-SOF control problem for the linear time invariant system $G_i(s)$ with the state-space realization of (1) is to find a gain matrix K_i ($u_i = K_i y_i$), such that the resulted closed-loop system is internally stable, and the H_∞ norm from w_i to z_i (Fig. 1) is smaller than γ, a specified positive number, i.e.

$$\|T_{z_i w_i}(s)\|_\infty < \gamma. \tag{2}$$

It is notable that the H_∞-SOF control problem can be transferred to a generalized SOF stabilization problem which is expressed via the following theorem (Cao, Lam, Sun, & Mao, 1998).

Theorem. *The system (A, B, C) is stabilizable via SOF if and only if there exist $P>0$, $X>0$ and K_i satisfying the following quadratic matrix inequality*

$$\begin{bmatrix} A^{\mathrm{T}}X + XA - PBB^{\mathrm{T}}X - XBB^{\mathrm{T}}P + PBB^{\mathrm{T}}P & (B^{\mathrm{T}}X + K_i C)^{\mathrm{T}} \\ B^{\mathrm{T}}X + K_i C & -I \end{bmatrix} < 0. \tag{3}$$

Here, the matrices A, B and C are constant and have appropriate dimensions. The X and P are symmetric and positive-definite matrices.

Since a solution for the consequent non convex optimization problem (3) cannot be directly achieved by using general and convex LMI techniques (Bevrani & Hiyama, 2007; Boyd, El Chaoui, Feron, & Balakrishnan, 1994; Swarnakar, Marquez, & Chen, 2007), a variety of methods were proposed by many researchers with many analytical and numerical methods to approach a local/global solution. In this paper, to solve the resulted SOF problem, an iterative LMI is used based on the existence necessary and sufficient condition for SOF stabilization, via the H_∞ control technique.

Using above theorem and the bounded real lemma (Zhou, Doyle, & Glover, 1996), the K_i is an H_∞-SOF controller for system (1), if and only if there exists $X>0$ such that

$$\bar{X}\bar{B}_i K_i \bar{C}_i + (\bar{X}\bar{B}_i K_i \bar{C}_i)^{\mathrm{T}} + \bar{A}_i^{\mathrm{T}}\bar{X} + \bar{X}\bar{A}_i < 0, \tag{4}$$

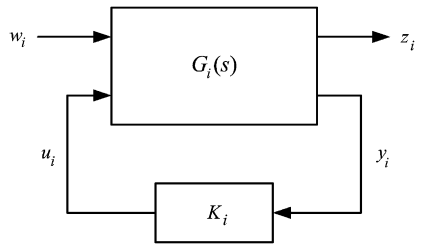

Fig. 1. Closed-loop system via H_∞-SOF control.

where

$$\bar{X}=\begin{bmatrix} X & 0 & 0\\ 0 & I & 0\\ 0 & 0 & I\end{bmatrix},\quad \bar{A}_i=\begin{bmatrix} A_i & B_{1i} & 0\\ 0 & -\gamma I/2 & 0\\ C_{1i} & 0 & -\gamma I/2\end{bmatrix},$$

$$\bar{B}_i=\begin{bmatrix} B_{2i}\\ 0\\ D_{12i}\end{bmatrix},\quad \bar{C}_i=[C_{2i}\ 0\ 0]. \tag{5}$$

Here, $\bar{A}_i, \bar{B}_i$ and $\bar{C}_i$ are three generalized matrices.

2.2. Modeling

In order to design a robust power system controller, it is first necessary to consider an appropriate linear mathematical description of multi-machine power system with two axis generator models. In the view point of "generator unit i", the nonlinear state space representation model for such a system has the form

$$\dot{x}_{gi}=f(x_{gi},u_{gi}), \tag{6}$$

where the states

$$x_{gi}^{\mathrm{T}}=[x_{1gi}\ x_{2gi}\ x_{3gi}\ x_{4gi}]=[\delta_i\ \omega_i\ E'_{qi}\ E'_{di}] \tag{7}$$

are defined as deviation form the equilibrium values

$$x_{egi}^{T}=[\delta_{1i}^{e}\ \omega_{2i}^{e}\ E'^{e}_{qi}\ E'^{e}_{di}]. \tag{8}$$

Using the linearization technique and after some manipulation, the nonlinear state Eqs. (6) can be expressed in the form of following linear state space model.

$$\dot{x}_{gi}=A_{gi}x_{gi}+B_{gi}u_{gi}, \tag{9}$$

where

$$A_{gi}=\begin{bmatrix} 0 & 1 & 0 & 0\\ a_{21} & -\dfrac{D_i}{M_i} & a_{23} & a_{24}\\ a_{31} & 0 & a_{33} & -\dfrac{G_{ii}\Delta x_{di}}{T'_{d0i}}\\ a_{41} & 0 & \dfrac{G_{ii}\Delta x_{qi}}{T'_{q0i}} & a_{44}\end{bmatrix},\quad B_{gi}=\begin{bmatrix} 0\\ 0\\ 1\\ \dfrac{1}{T'_{d0i}}\\ 0\end{bmatrix} \tag{10}$$

and

$$\Delta x_{di}=x_{di}-x'_{di},\quad \Delta x_{qi}=x_{qi}-x'_{di}. \tag{11}$$

The a_{kj} elements are described in Appendix. The other parameters are defined as follows. δ_i, Machine rotor angle; ω_i, Machine rotor speed; E'_{di}, d axis internal machine voltage; E'_{qi}, q axis internal machine voltage; D_i, Damping constant; M_i, Inertia constant; G_{ii}, Driving point conductance; T'_{doi}, d axis open circuit transient time constant; T'_{qoi}, q axis open circuit transient time constant; x_{di}, d axis synchronous reactance; x'_{di}, d axis transient reactance; x_{qi}, q axis synchronous reactance.

Considering the conventional AVR–PSS system, the overall system control input can be written in the following form.

$$u_{gi}=u_{ci}+u_i, \tag{12}$$

where, u_{ci} is the output of conventional AVR–PSS system and the u_i is the new control input (Fig. 2). Therefore, the overall system can be described as follows:

$$\dot{x}_i=A_ix_i+B_iu_i \tag{13}$$

and

$$x_i^{\mathrm{T}}=[x_{gi_{1\times 4}}^{\mathrm{T}}\ \ x_{ci_{1\times m}}^{\mathrm{T}}]_{1\times(4+m)}. \tag{14}$$

Here, the x_{ci} shows the state vector of conventional AVR–PSS system and m represents its dynamic order.

2.3. Proposed control framework

The overall control structure using SOF control design for an assumed power system is shown in Fig. 2, where blocks PSS and AVR represents the existing conventional power system stabilizer and voltage regulators. Here, the electrical power signal Δp_{ei} is considered as input signal for the PSS unit. The optimal gain vector (OGV) uses the terminal voltage Δv_{ti}, electrical power Δp_{ei} and machine speed $\Delta\omega_i$ as input signals. The Δv_{refi} and d_i show the reference voltage deviation and system disturbance input, respectively.

Using the linearized model for power system "i" in the form of (1) and performing the standard H_∞-SOF configuration with considering appropriate controlled output signals results an effective control framework,

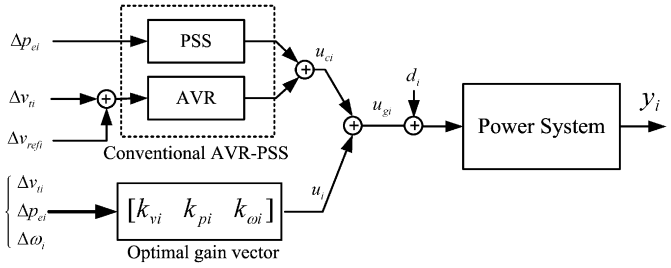

Fig. 2. Overall control structure.

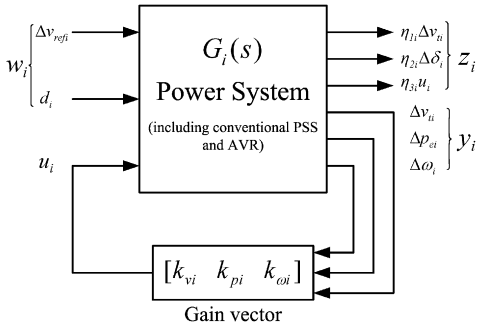

Fig. 3. The proposed H_∞-SOF control framework.

which is shown in Fig. 3. This control structure adapts the H_∞-SOF control technique with the described power system control targets and allows a direct trade-off between voltage regulation and closed-loop stability by merely tuning of a vector gain.

Here, disturbance input vector w_i, controlled output vector z_i and measured output vector y_i are considered as follows:

$$w_i^T = [\Delta v_{refi} \;\; d_i], \tag{15}$$

$$z_i^T = [\eta_{1i}\Delta v_{ti} \;\; \eta_{2i}\Delta\delta_i \;\; \eta_{3i}u_i], \tag{16}$$

$$y_i^T = [\Delta v_{ti} \;\; \Delta p_{ei} \;\; \Delta\omega_i]. \tag{17}$$

The Δv_{ti} and Δp_{ei} can be easily expressed via the specified system states, and the η_{1i}, η_{2i} and η_{3i} are constant weights that must be chosen by the designer to achieve a desired closed-loop performance. Since the vector z_i properly covers all significant controlled signals which must be minimized by an ideal AVR–PSS design, it is expected that the proposed robust controller should be able to satisfy the voltage regulation and stabilizing objectives, simultaneously. It is notable that, since the solution must be obtained trough the minimizing of an $H\infty$ optimization problem, the designed feedback system satisfies the robust stability and voltage regulation performance for the overall closed-loop system. Moreover, the developed ILMI algorithm (which is described in the next section) provides an effective and flexible tool for finding an appropriate solution in the form of a simple static gain controller.

2.4. ILMI algorithm

It is well-known that static output feedback stabilization is still an open problem. Its reformulation generally leads to bilinear matrix inequalities (BMI) which are non-convex. This kind of problem is usually solved by an iterative algorithm that may not converge to an optimal solution.

Here, in order to solve the H_∞-SOF, an iterative LMI algorithm has been used. The algorithm is mainly based on the given idea by Cao et al. (1998). The key point is to formulate the H_∞ problem via a generalized static output stabilization feedback such that all eigenvalues of (A-B K_i C) shift towards the left half plane in the complex s-plane, to close to feasibility of (3). The described theorem in the previous section gives a family of internally stabilizing SOF gains is defined as K_{sof}. The desirable solution K_i is an admissible SOF law

$$u_i = K_i y_i, \quad K_i \in K_{sof}, \tag{18}$$

such that

$$\|T_{ziwi}(s)\|_\infty < \gamma^*, \quad |\gamma - \gamma^*| < \varepsilon, \tag{19}$$

where ε is a small positive number. The performance index γ^* indicates a lower bound such that the closed-loop system is $H\infty$ stabilizable. The optimal performance index (γ), can be obtained from the application of a full dynamic H_∞ dynamic output feedback control method. The proposed algorithm, which gives an iterative LMI solution for above optimization problem includes the following steps:

Step 1. Set initial values and compute the generalized system $(\bar{A}_i, \bar{B}_i, \bar{C}_i)$ as shown in (5), for the given power system including conventional AVR–PSS system. For this purpose, according to (13), the matrix A_i has the following form and the elements of other matrices in (5) can be obtained based on the structure of the used excitation system and AVR–PSS unit.

$$A_i = \begin{bmatrix} A_{gi_{(4\times4)}} & 0_{(4\times m)} \\ 0_{(m\times4)} & A_{ci_{(m\times m)}} \end{bmatrix}. \tag{20}$$

The "c" is used for the conventional AVR–PSS system.

Step 2. Set $i = 1$, $\Delta\gamma = \Delta\gamma_0$ and let $\gamma_i = \gamma_0 > \gamma$. $\Delta\gamma_0$ and γ_0 are positive real numbers.

Step 3. Select $Q > 0$, and solve $\bar{X}$ from the following algebraic Riccati equation

$$\bar{A}_i^T\bar{X} + \bar{X}\bar{A}_i - \bar{X}\bar{B}_i\bar{B}_i^T\bar{X} + Q = 0. \tag{21}$$

Set $P_1 = \bar{X}$.

Step 4. Solve the following optimization problem for $\bar{X}_i$, K_i and a_i.

Minimize a_i subject to the LMI constraints:

$$\begin{bmatrix} \bar{A}_i^T\bar{X}_i + \bar{X}_i\bar{A}_i - P_i\bar{B}_i\bar{B}_i^T\bar{X}_i - \bar{X}_i\bar{B}_i\bar{B}_i^TP_i + P_i\bar{B}_i\bar{B}_i^TP_i - a_i\bar{X}_i & (\bar{B}_i^T\bar{X}_i + K_i\bar{C}_i)^T \\ \bar{B}_i^T\bar{X}_i + K_i\bar{C} & -I \end{bmatrix} < 0, \tag{22}$$

$$\bar{X}_i = \bar{X}_i^T > 0. \tag{23}$$

Denote a_i^* as the minimized value of a_i.

Step 5. If $a_i^* \leqslant 0$, go to step 8.

Step 6. For $i > 1$, if $a_{i-1}^* \leqslant 0$, $K_{i-1} \in K_{sof}$ is an H_∞ controller and $\gamma^* = \gamma_i + \Delta\gamma$ indicates a lower bound such that the above system is H_∞ stabilizable via SOF control. Go to step 10.

Step 7. If $i = 1$, solve the following optimization problem for $\bar{X}_i$ and K_i.

Minimize trace($\bar{X}_i$) subject to the above LMI constraints (22) and (23) with $a_i = a_i^*$. Denote $\bar{X}_i^*$ as the $\bar{X}_i$ that minimized trace($\bar{X}_i$). Go to step 9.

Step 8. Set $\gamma_i = \gamma_i - \Delta\gamma$, $i = i+1$. Then do steps 3 to 5.

Step 9. Set $i = i+1$ and $P_i = \bar{X}_{i-1}^*$, then go to step 4.

Step 10. If the obtained solution (K_{i-1}) satisfies the gain constraint, it is desirable, otherwise change constant weights (η_i) and go to step 1.

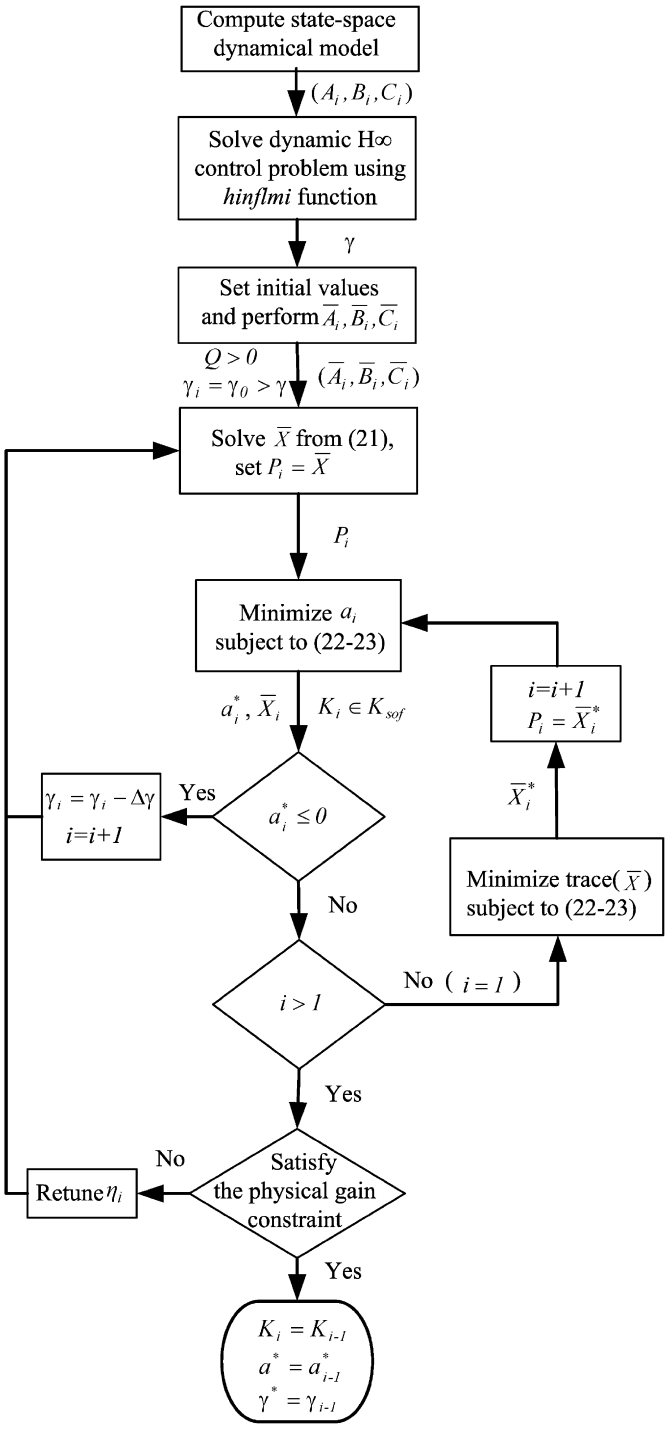

Fig. 4. Iterative LMI algorithm.

The proposed iterative LMI algorithm, which is summarized in the flowchart of Fig. 4, shows that if one simply perturbs $\bar{A}_i$ to $\bar{A}_i - (a/2)I$ for some $a>0$, a solution of the matrix inequality (3) can be obtained for the performed generalized plant. That is, there exist a real number ($a>0$) and a matrix $P>0$ to satisfy inequality (22). Consequently, the closed-loop system matrix $\bar{A}_i - \bar{B}_i K \bar{C}_i$ has eigenvalues on the left-hand side of the line $\Re(s) = a$ in the complex s-plane. Based on the idea that all eigenvalues of $\bar{A}_i - \bar{B}_i K \bar{C}_i$ are shifted progressively towards the left half plane through the reduction of a. The given generalized eigenvalue minimization in the proposed iterative LMI algorithm guarantees this progressive reduction.

2.5. Weights selection

The vector $\eta_i = [\eta_{1i}\ \eta_{2i}\ \eta_{3i}]$ is a constant weight vector that must be chosen by the designer to get the desired closed-loop performance. The selection of these weights is dependent on specified voltage regulation and damping performance goals. In fact an important issue with regard to selection of these weights is the degree to which they can guarantee the satisfaction of design performance objectives. It is notable that η_{3i} sets a limit on the allowed control signal to penalize fast changes, large overshoot with a reasonable control gain to meet the physical constraints. Therefore, the selection of constant weights entails a compromise among several performance requirements.

One can simply fix the weights to unity and use the method with regional pole placement technique for performance tuning (Gahinet & Chilali, 1996). Here, for the sake of weight selection, the following steps are simply considered through the proposed ILMI algorithm:

Step 1. Set initial values, e.g. [1 1 1].

Step 2. Run the ILMI algorithm (summarized in Fig. 4).

Step 3. If the ILMI algorithm gives a feasible solution such that satisfies the robust H_∞ performance and the gain constraint; the assigned weights vector is acceptable. Otherwise retune η_i and go to Step 2.

3. Real time implementation

To illustrate the effectiveness of the proposed control strategy, a real time experiment has been performed on the large scale Analog Power System Simulator at the Research Laboratory of the Kyushu Electric Power Company. For the purpose of this study, a longitudinal four-machine infinite bus system is considered as a test system. A single line representation of the study system is shown in Fig. 5. Although, in the given model the number

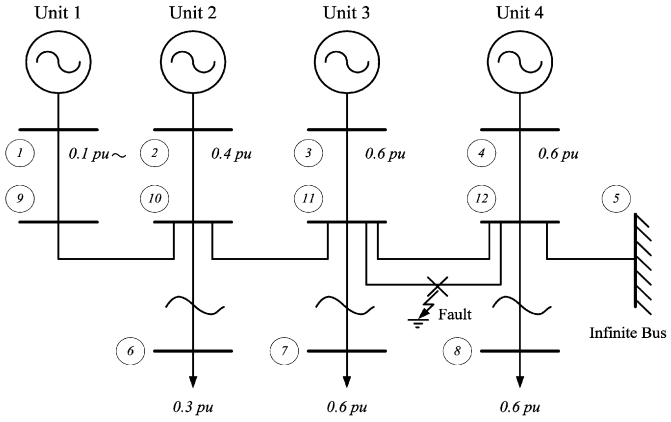

Fig. 5. Four-machine infinite-bus power system.

of generators is reduced to four, it closely represents the dynamic behavior of the west part of Japan (West Japan Power System), and it is widely used by researchers (Bevrani & Hiyama, 2007; Hiyama, Oniki, & Nagashima, 1996; Hiyama, Kawakita, & Ono, 2004; Hiyama, Kojima, Ohtsu, & Furukawa, 2005). The most important global and local oscillation modes of actual system are included. For the study system, the local mode for each corresponding unit, and the low frequency global mode are around 1.5 Hz and 0.3 Hz, respectively. Each unit is a thermal unit, and has a separately conventional excitation control system as shown in Figs. 6a and b.

Each unit has a full set of governor-turbine system (governor, steam valve servo-system, high-pressure turbine, intermediate-pressure turbine, and low-pressure turbine) which is shown in Fig. 7. The generators, lines, conventional excitation system and governor-turbine parameters are given in Tables 1–4, respectively.

Unit 1 is selected to be equipped with robust control, and therefore our objective is to apply the control strategy described in the previous section to controller design for unit 1. The whole power system has been implemented in the mentioned laboratory. Fig. 8 shows the overview of the applied laboratory experiment devices including the

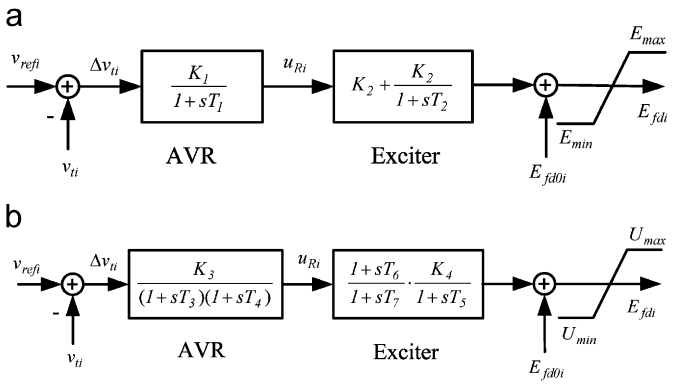

Fig. 6. Conventional excitation control system: (a) for units 2 and 3 and (b) for units 1 and 4.

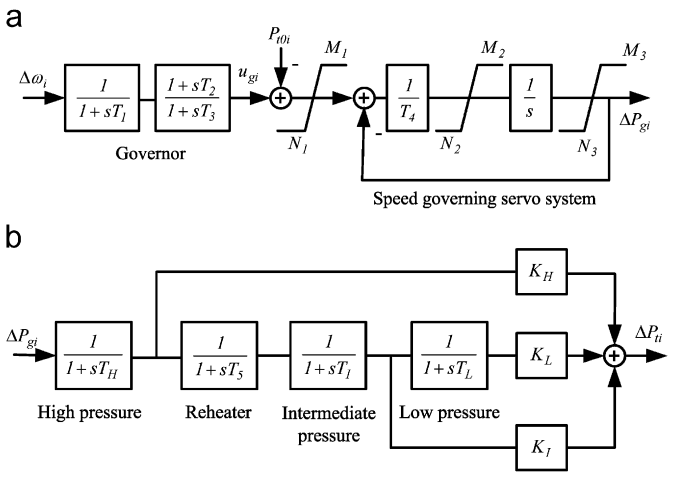

Fig. 7. (a) Conventional speed governing system and (b) detailed turbine system.

Table 1
Generator constants

Unit no.	M_i (s)	D_i	x_{di} (pu)	x'_{di} (pu)	x_{qi} (pu)	x'_{qi} (pu)	T'_{d0i} (s)	T'_{q0i} (s)	MVA
1	8.05	0.002	1.860	0.440	1.350	1.340	0.733	0.0873	1000
2	7.00	0.002	1.490	0.252	0.822	0.821	1.500	0.1270	600
3	6.00	0.002	1.485	0.509	1.420	1.410	1.550	0.2675	1000
4	8.05	0.002	1.860	0.440	1.350	1.340	0.733	0.0873	900

Table 2
Line parameters

Line no.	Bus–Bus	R_{ij} (pu)	X_{ij} (pu)	S_{ij} (pu)
1	1–9	0.02700	0.1304	0.0000
2	2–10	0.07000	0.1701	0.0000
3	3–11	0.04400	0.1718	0.0000
4	4–12	0.02700	0.1288	0.0000
5	10–6	0.02700	0.2238	0.0000
6	11–7	0.04000	0.1718	0.0000
7	12–8	0.06130	0.2535	0.0000
8	9–10	0.01101	0.0829	0.0246
9	10–11	0.01101	0.0829	0.0246
10	11–12	0.01468	0.1105	0.0328
11	12–5	0.12480	0.9085	0.1640

Table 3
Excitation parameters

K_1	K_2	K_3	K_4	$\lvert E_{max(min)}\rvert$	U_{max}	U_{min}
1.00	19.21	10.00	6.48	5.71	7.60	−5.20
T_1 (s)	T_2 (s)	T_3 (s)	T_4 (s)	T_5 (s)	T_6 (s)	T_7 (s)
0.010	1.560	0.013	0.013	0.200	3.000	10.000

Table 4
Governor and turbine parameters

Parameters	Unit 1	Unit 2	Unit 3	Unit 4
T_1 (s)	0.08	0.06	0.07	0.07
T_2 (s)	0.10	0.10	0.10	0.10
T_3 (s)	0.10	0.10	0.10	0.10
T_4 (s)	0.40	0.36	0.42	0.42
T_5 (s)	10.0	10.0	10.0	10.0
T_H (s)	0.05	0.05	0.05	0.05
T_I (s)	0.08	0.08	0.08	0.08
T_L (s)	0.58	0.58	0.58	0.58
K_H (pu)	0.31	0.31	0.31	0.31
K_I (pu)	0.24	0.24	0.24	0.24
K_L (pu)	0.45	0.45	0.45	0.45
M_1 (pu/min)	0.50	0.50	0.50	0.50
M_2 (pu/Min)	0.20	0.20	0.20	0.20
M_3 (pu/Min)	1.50	1.50	1.50	1.50
N_1 (pu/Min)	−0.50	−0.50	−0.50	−0.50
N_2 (pu/Min)	−0.20	−0.20	−0.20	−0.20
N_3 (pu/Min)	−0.50	−0.50	−0.50	−0.50

a

b

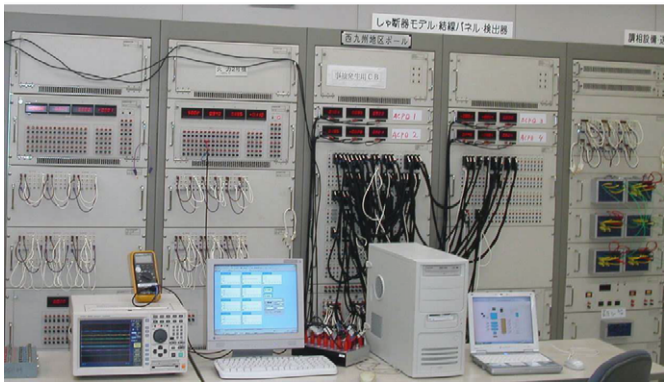

Fig. 8. Performed laboratory experiment: (a) overview of analog power system simulator and (b) the control/monitoring desks.

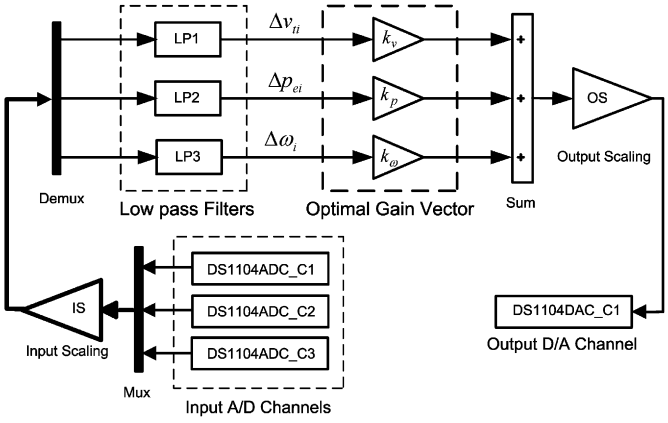

Fig. 9. The performed computer based control loop.

control/monitoring desks. A digital oscilloscope and a notebook computer (shown in Fig. 8b) are used for monitoring purposes.

The proposed control loop (Fig. 9) has been built in a personal computer were connected to the power system using a digital signal processing (DSP) board equipped with analog to digital (A/D) and digital to analog (D/A) converters as the physical interfaces between the personal computer and the analog power system hardware. In Fig. 9, the input/output scaling blocks are used to match the PC based controller and the Analog Power System hardware, signally. High frequency noises are removed by appropriate low pass filters.

Then, applying the proposed H_∞-SOF control methodology an OGV for the problem at hand is obtained as follows:

$$K_{1,\mathrm{SOF}} = [9.5899 \;\; 7.8648 \;\; 1.2990]. \quad (24)$$

The considered constraints on limiters and control loop gains are set according to the real power system control units and close to ones that exist for the conventional AVR–PSS units. The used constant weight vector (η_i) is given in Appendix.

4. Experiment results

The performance of the closed-loop system using the proposed OGV in comparison of a pure conventional AVR–PSS system is tested in the presence of voltage deviation, faults and system disturbance. The configuration of the applied conventional power system stabilizer, which was accurately tuned by the system operators, is illustrated in Fig. 10. The conventional PSS parameters are listed in Table 5.

During the first test scenario, the output setting of unit 1 is fixed to 0.5 pu. Fig. 11 shows the electrical power, terminal voltage and machine speed of unit 1, following a fault on the line between buses 11 and 12 at 2 s. To force a more critical situation, the faulted line is isolated from the network just after four cycles from the fault. It can be seen that the system response is quite improved using the designed feedback gains.

Furthermore, the size of resulted stable region by the proposed method is significantly enlarged in comparison of conventional AVR–PSS controller. To show this fact, the critical power output from unit 1 in the presence of a three-phase to ground fault is considered as a good measure. To investigate the critical point, the real power output of unit 1 is increased from 0.3 pu (The setting of the real power output from the other units is fixed at the values shown in Fig. 5). Using the conventional AVR–PSS structure, the resulted critical power output from unit 1 to be 0.31 pu

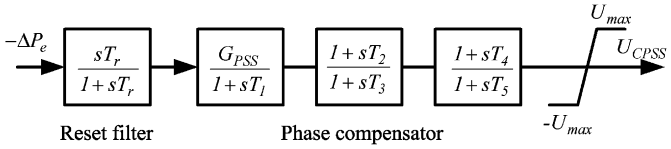

Fig. 10. Conventional power system stabilizer.

Table 5
Conventional PSS parameters

T_r (s)	G_{PSS}	$U_{\max}$ (pu)	T_1 (s)
5.00	10.00	1.00	0.025
T_2 (s)	T_3 (s)	T_4 (s)	T_5 (s)
0.056	0.054	0.037	0.53

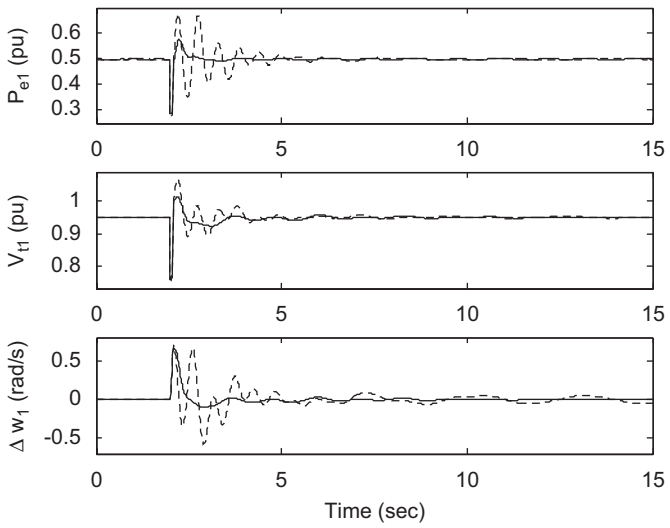

Fig. 11. System response for a fault between buses 11 and 12. Solid (using OGV), dotted (conventional AVR–PSS).

Table 6
Critical power output of unit 1

Control design	Critical power output
Proposed design	0.94 (pu)
Conventional AVR–PSS	0.52 (pu)

(Hiyama et al., 1996, 2004); and in case of tight tuning of CPSS parameters it could not be higher than 0.52 pu. For the proposed control method, the critical power output, as shown in Table 6, is increased to 0.94 pu. The system response for a fault between buses 11 and 12, while the output setting of unit 1 is increased to 0.7 pu is shown in Fig. 12.

In the second test case, the performance of designed controllers was evaluated in the presence of a 0.05 pu step disturbance injected at the voltage reference input of unit 1 at 20 s. Fig. 13 shows the closed-loop response of the power systems fitted with the conventional control and the proposed robust control design. Better performance is achieved by the proposed control strategy. In the next scenario, the closed-loop system response is examined in the face of a step disturbance (d_i) at 20 s. The result is shown in Fig. 14. Comparing the experiment results shows that the robust design achieves robustness against the voltage deviation, disturbance and line fault with a quite good voltage regulation and damping performance.

Finally, to demonstrate the simultaneous damping of local (fast) and global (slow) oscillation modes, filtering analysis has been performed. The laboratory results for the speed deviation of unit 1, following a fault on the line between buses 11 and 12 are shown in Fig. 15 (in this experiment, the fault was happen at 2 s and the output setting of unit 1 was fixed at 0.45 pu).

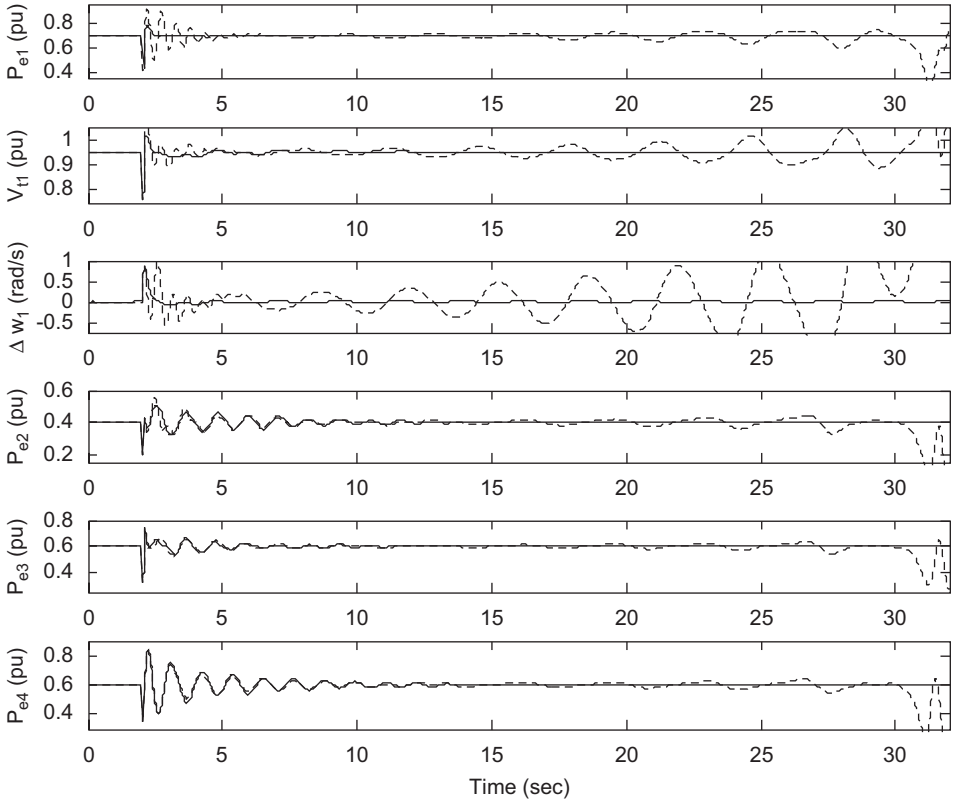

Fig. 12. System response for a fault between buses 11 and 12, while the output setting of unit 1 is fixed to 0.5 pu. Solid (using OGV), dotted (conventional AVR–PSS).

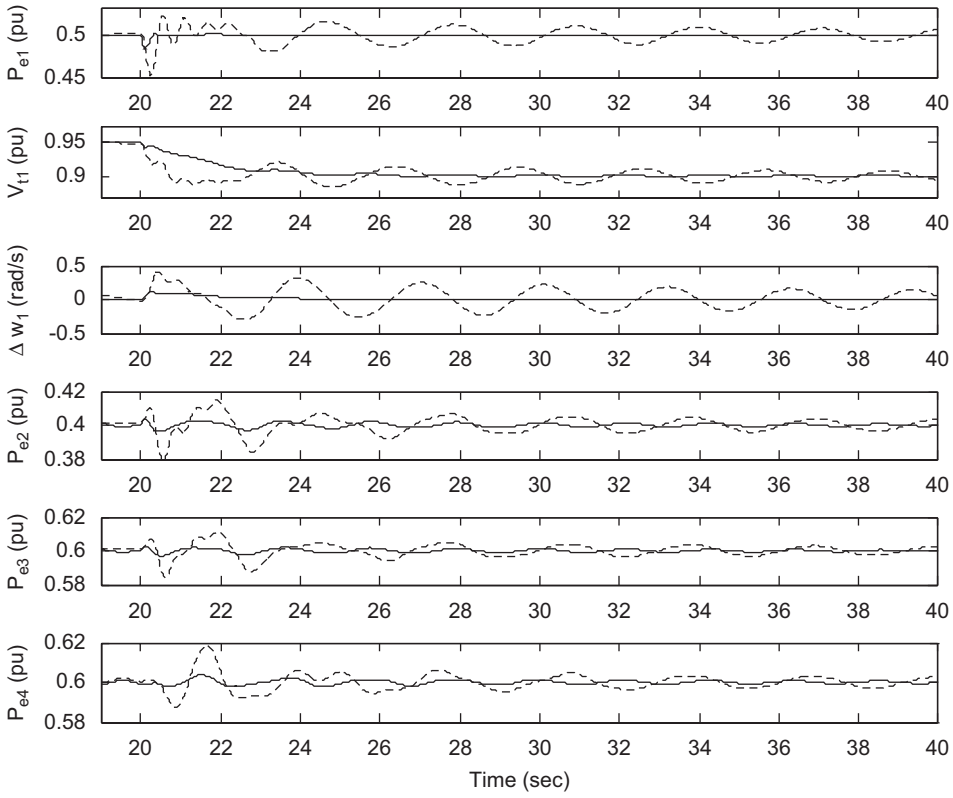

Fig. 13. System response for a 0.05 pu step change at the voltage reference input of unit 1. Solid (using OGV), dotted (conventional AVR–PSS).

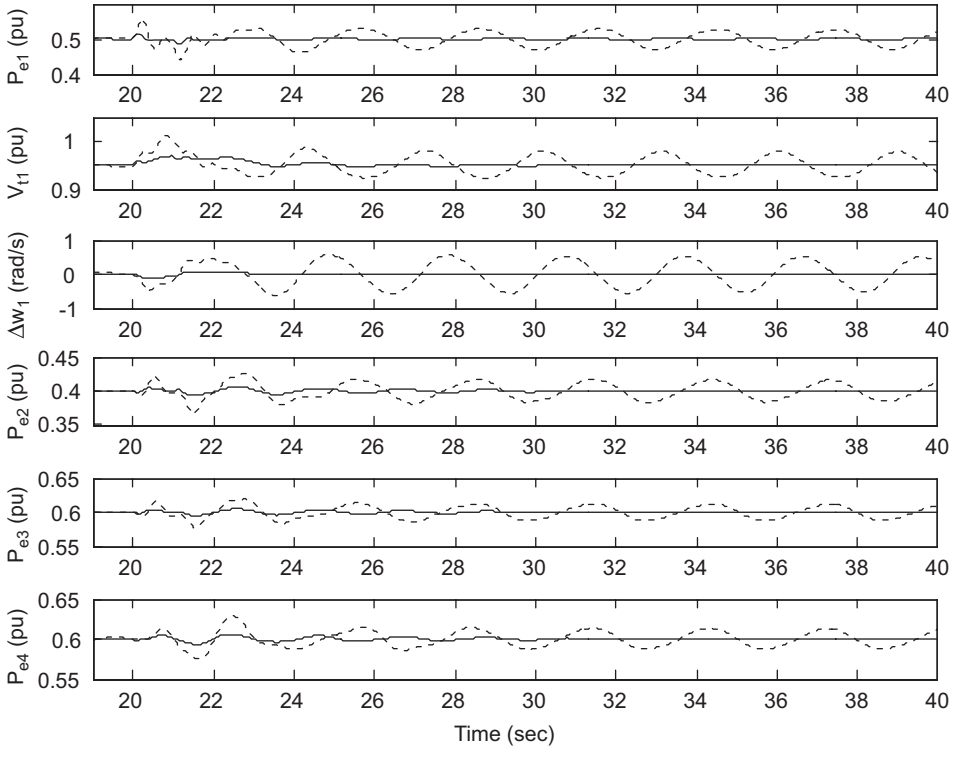

Fig. 14. System response for a step disturbance at 20 s. Solid (using OGV), dotted (conventional AVR–PSS).

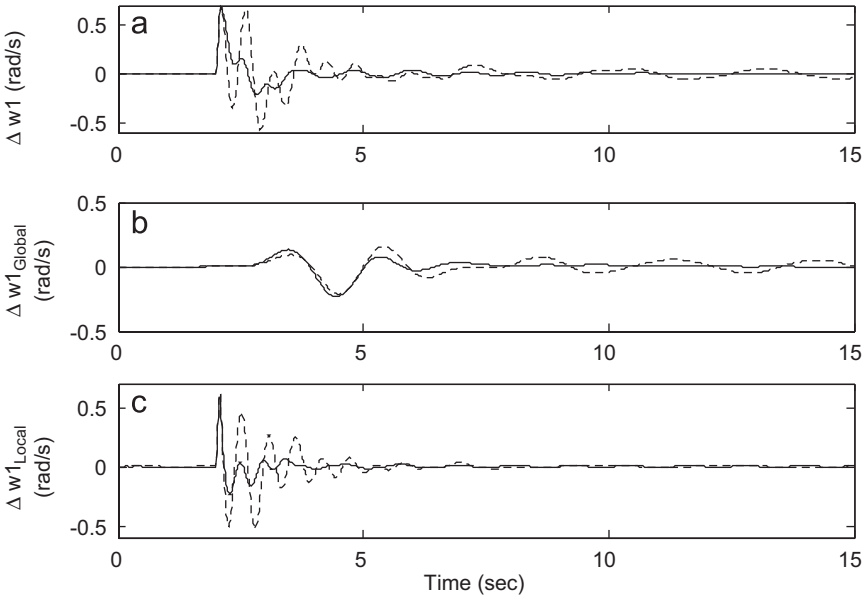

Fig. 15. Oscillation modes analysis following a fault: (a) speed deviation, (b) global mode and (c) fast mode. Solid (using OGV), dotted (conventional AVR–PSS).

5. Conclusion

In order to achieve simultaneous enhancement of power system stability and voltage regulation, a new control strategy is developed using an H_∞-SOF control technique and a developed iterative LMI algorithm. The proposed method was applied to a four-machine infinite bus power system, through a laboratory real-time experiment, and the results are compared with a conventional AVR–PSS design. The performance of the resulting closed-loop system is shown to be satisfactory over a wide range of operating conditions.

As shown in the nonlinear real-time simulation results, the proposed coordination through a new optimal feedback loop has brought a significant improvement to power system performance and has increased the stable region of operation. The resulting controller is not only robust but it also allows direct effective trade-off between voltage regulation and damping performance. Furthermore, because of simplicity of structure, decentralized property, ease of formulation and flexibility, the design methodology can be practically implemented.

Acknowledgments

This work was supported in part by the Research Office at the University of Kurdistan (Iran) and in part by the Japan Society for the promotion of Science (JSPS) under grant P04346. The authors would like to thank S. Wakasugi, A. Matsunaga, Y. Fujimoto, T. Kouichi, Y. Hirofumi and K. Hiroyuki for their helps to make a successful experiment in Research Laboratory of the Kyushu Electric Power Company. Also, the authors thank Dr. J. J. Ford from Queensland University of Technology (Australia) for his help to prepare the final version of this paper.

Appendix

The nonlinear model of (6) can be presented as follows:

$$\dot{x}_{1gi} = x_{2gi},$$
$$\dot{x}_{2gi} = -(D_i/M_i)x_{2gi} - (1/M_i)\Delta P_{ei}(x),$$
$$\dot{x}_{3gi} = -(1/T'_{d0i})x_{3gi} - (\Delta x_{di}(x)/T'_{d0i})\Delta I_{di}(x) + u_{gi},$$
$$\dot{x}_{4gi} = -(1/T'_{q0i})x_{4gi} - (\Delta x_{qi}(x)/T'_{q0i})\Delta I_{qi}(x),$$

where

$$\Delta P_{ei}(x) = (E'_{di}I_{di} + E'_{qi}I_{qi}) - (E'^{e}_{di}I^{e}_{di} + E'^{e}_{qi}I^{e}_{qi}),$$

$$I_{di} = \sum_k [G_{ik}\cos\delta_{ik} + B_{ik}\sin\delta_{ik}]E'_{dk} + \sum_k [G_{ik}\sin\delta_{ik} - B_{ik}\cos\delta_{ik}]E'_{qk},$$

$$I_{qi} = \sum_k [B_{ik}\cos\delta_{ik} - G_{ik}\sin\delta_{ik}]E'_{dk} + \sum_k [G_{ik}\cos\delta_{ik} + B_{ik}\sin\delta_{ik}]E'_{qk}.$$

A detailed description of all symbols and quantities can be found in Sauer and Pai (1998). The elements of A_{gi} matrix in (10) are

$$a_{21} = -\frac{1}{M_i}\frac{\partial f_{1i}(x)}{\partial x_{1gi}}\bigg|_{x_{egi}}$$

$$a_{23} = -\frac{[G_{ii}E'^{e}_{qi} - B_{ii}E'^{e}_{di} + I^{e}_{qi}]}{M_i} - \frac{1}{M_i}\frac{\partial f_{1i}(x)}{\partial x_{3gi}}\bigg|_{x_{egi}},$$

$$a_{24} = -\frac{[G_{ii}E'^{e}_{di} + B_{ii}E'^{e}_{qi} + I^{e}_{di}]}{M_i} - \frac{1}{M_i}\frac{\partial f_{1i}(x)}{\partial x_{4gi}}\bigg|_{x_{egi}},$$

$$a_{31} = -\frac{\Delta x_{di}}{T'_{d0i}}\frac{\partial f_{2i}(x)}{\partial x_{1gi}}\bigg|_{x_{egi}}, \quad a_{33} = -\frac{1}{T'_{d0i}} + \frac{B_{ii}\Delta x_{di}}{T'_{d0i}},$$

$$a_{41} = -\frac{\Delta x_{qi}}{T'_{q0i}}\frac{\partial f_{3i}(x)}{\partial x_{1gi}}\bigg|_{x_{egi}}, \quad a_{44} = -\frac{1}{T'_{q0i}} + \frac{B_{ii}\Delta x_{qi}}{T'_{q0i}},$$

where

$$\begin{aligned} f_{1i}(x) = {} & x_{4gi}\Delta I_{di}(x) + x_{3gi}\Delta I_{qi}(x) \\ & + \sum_{k\neq i}\{[E'^{e}_{di}\eta_{ik}(\delta) + E'^{e}_{qi}\hat{\eta}_{ik}(\delta)]x_{4gk} \\ & + [E'^{e}_{di}v_{ik}(\delta) + E'^{e}_{qi}\hat{v}_{ik}(\delta)]x_{3gk} \\ & + [E'^{e}_{di}\upsilon_{ik}(\delta) + E'^{e}_{qi}\hat{\upsilon}_{ik}(\delta)]\sin\phi_{ik}\}, \end{aligned}$$

$$f_{2i}(x) = \sum_{k\neq i}[\eta_{ik}(\delta)x_{4gk} + v_{ik}(\delta)x_{3gk} + \upsilon_{ik}(\delta)\sin\phi_{ik}],$$

$$f_{3i}(x) = \sum_{k\neq i}[\hat{\eta}_{ik}(\delta)x_{4gk} + \hat{v}_{ik}(\delta)x_{3gk} + \hat{\upsilon}_{ik}(\delta)\sin\phi_{ik}],$$

$$\eta_{ik}(\delta) = G_{ik}\cos\delta_{ik} + B_{ik}\sin\delta_{ik},$$
$$\hat{\eta}_{ik}(\delta) = B_{ik}\cos\delta_{ik} - G_{ik}\sin\delta_{ik},$$

$$v_{ik}(\delta) = G_{ik}\sin\delta_{ik} - B_{ik}\cos\delta_{ik},$$
$$\hat{v}_{ik}(\delta) = B_{ik}\sin\delta_{ik} - G_{ik}\cos\delta_{ik},$$

$$\upsilon_{ik}(\delta) = 2g1_{ik}\sin\frac{\delta^{e}_{ik} + \delta_{ik}}{2} + 2g2_{ik}\cos\frac{\delta^{e}_{ik} + \delta_{ik}}{2},$$
$$\phi_{ik} = 0.5(x_{1gi} - x_{1gk}),$$

$$\hat{\upsilon}_{ik}(\delta) = 2g2_{ik}\sin\frac{\delta^{e}_{ik} + \delta_{ik}}{2} - 2g1_{ik}\cos\frac{\delta^{e}_{ik} + \delta_{ik}}{2},$$
$$\delta_{ik} = \delta_i - \delta_k,$$

$$g1_{ik} = G_{ik}E'^{e}_{dk} - B_{ik}E'^{e}_{qk},$$
$$g2_{ik} = G_{ik}E'^{e}_{qk} + B_{ik}E'^{e}_{qk},$$

Constant weights : $\eta_1 = [0.25 \;\; 0.1 \;\; 5]$.

References

Bevrani, H., & Hiyama, T. (2006). Stability and voltage regulation enhancement using an optimal gain vector. In *Proceedings of IEEE PES general meeting*, Canada.

Bevrani, H., & Hiyama, T. (2007). Robust load–frequency regulation: a real-time laboratory experiment. *Optimal Control Applications and Methods*, *28*(6), 419–433.

Boyd, S. P., El Chaoui, L., Feron, E., & Balakrishnan, V. (1994). *Linear matrix inequalities in systems and control theory*. Philadelphia, PA: SIAM.

Cao, Y. Y., Lam, J., Sun, Y. X., & Mao, W. J. (1998). Static output feedback stabilization: An ILMI approach. *Automatica*, *34*(12), 1641–1645.

Gahinet, P., & Chilali, M. (1996). H_∞-design with pole placement constraints. *IEEE Transactions on Automatic Control*, *41*(3), 358–367.

Guo, Y., Hill, D. J., & Wang, Y. (2001). Global transient stability and voltage regulation for power systems. *IEEE Transactions on Power Systems*, *16*(4), 678–688.

Heniche, A., Bourles, H., & Houry, M. P. (1995). A desensitized controller for voltage regulation of power systems. *IEEE Transactions on Power Systems*, *10*(3), 1461–1466.

Hiyama, T., Kawakita, M., & Ono, H. (2004). Multi-agent based wide area stabilization control of power systems using power system stabilizer. In *Proceedings of IEEE international conference on power system technology*.

Hiyama, T., Kojima, D., Ohtsu, K., & Furukawa, K. (2005). Eigenvalue-based wide area stability monitoring of power systems. *Control Engineering Practice*, *13*, 1515–1523.

Hiyama, T., Oniki, S., & Nagashima, H. (1996). Evaluation of advanced fuzzy logic PSS on analog network simulator and actual installation on hydro generators. *IEEE Transactions on Energy Conversion*, *11*(1), 125–131.

Kundur, P., Paserba, J., Ajjarapu, V., Andersson, G., Bose, A., Canizares, C., et al. (2004). Definition and classification of power system stability. *IEEE Transactions on Power Systems*, *19*(2), 1387–1401.

Law, K. T., Hill, D. J., & Godfrey, N. R. (1994a). Robust co-ordinated AVR–PSS design. *IEEE Transactions on Power Systems*, *9*(3), 1218–1225.

Law, K. T., Hill, D. J., & Godfrey, N. R. (1994b). Robust controller structure for coordinated power system voltage regulator and stabilizer design. *IEEE Transactions on Control Systems Technology*, *2*(3), 220–232.

Malik, O. P., Hope, G. S., Gorski, Y. M., Uskakov, V. A., & Rackevich, A. L. (1986). Experimental studies on adaptive microprocessor stabilizers for synchronous generators. *IFAC power system and power plant control* (pp. 125–130). Beijing, China.

Sauer, P. W., & Pai, M. A. (1998). *Power system dynamic and stability*. Englewood Cliffs, NJ: Prentice-Hall.

Soliman, H. M., & Sakar, M. M. F. (1988). Wide-range power system pole placer. *Institute of Electrical Engineering Proceedings, Part C*, *135*(3), 195–200.

Swarnakar, A., Marquez, H. J., & Chen, T. (2007). Robust stabilization of nonlinear interconnected systems with application to an industrian utility boiler. *Control Engineering Practice*, *15*(6), 639–654.

Venikov, V. A., & Stroev, V. A. (1971). Power system stability as affected by automatic control of generators—some methods of analysis and synthesis. *IEEE Transactions on PAS*, *PAS-90*, 2483–2487.

Wang, Y., & Hill, D. J. (1996). Robust nonlinear coordinated control of power systems. *Automatica*, *32*(4), 611–618.

Yadaiah, N., Kumar, A. G. D., & Bhattacharya, J. L. (2004). Fuzzy based coordinated controller for power system stability and voltage regulation. *Electric Power System Research*, *69*, 169–177.

Zhou, K., Doyle, J. C., & Glover, K. (1996). *Robust and optimal control*. New Jersey: Prentice-Hall.